
Supporting Information

(24 pages including the cover page)

**Base–Controlled Directed Synthesis of Metal–Methyleneimidazoline
(MIZ) and Metal–Mesoionic Carbene (MIC) Compounds**

Mandeep Kaur, Kamaless Patra, Noor U Din Reshi and Jitendra K. Bera*

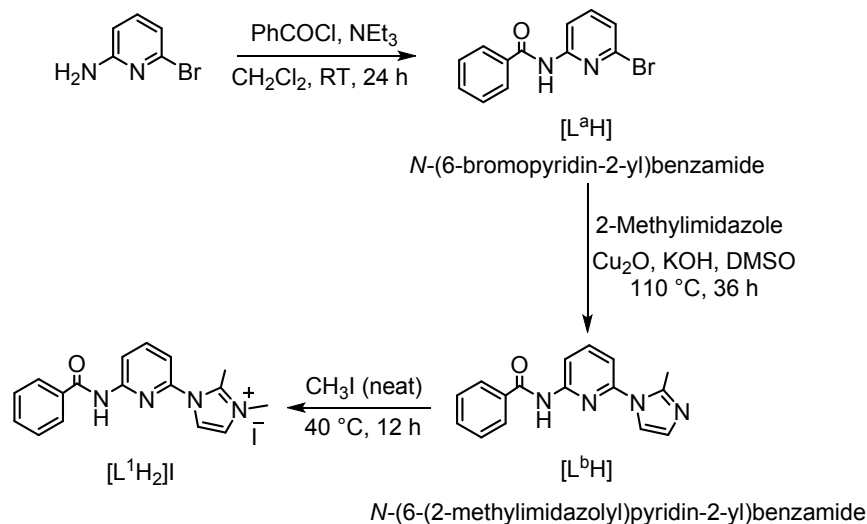
Department of Chemistry and Center for Environmental Science and Engineering, Indian
Institute of Technology Kanpur, Kanpur, 208016, India

E-mail: jbera@iitk.ac.in

Contents

	Page No.
Scheme S1. Synthesis of $[L^1H_2]I$	S3
Figure S1. Molecular structure of $[L^1H_2]I$	S3
Figure S2-S9. 1H and ^{13}C NMR spectra of $[L^1H_2]I$ and $[L^2H]I$	S4-S7
Figure S10-S25 1H and ^{13}C NMR spectra of 1 - 8	S8-S15
Figure S26-S35 ESI-MS of 1 - 8	S16-S20
Figure S36-S37 Molecular structures of 4 and 6	S21
Table S1-S2 Crystallographic data and pertinent refinement parameters	S22-S23
Optimized structures	S24
Cartesian coordinates for the computed geometries	S25-S37

Synthesis of $[L^1H_2]I$



Scheme S1. Synthesis of the ligand $[L^1H_2]I$.

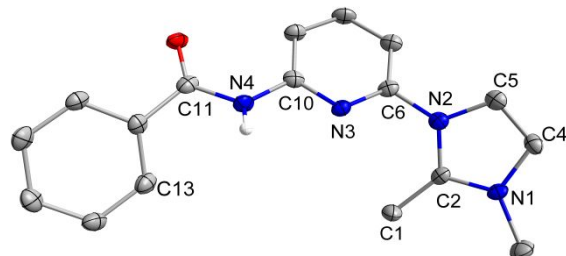
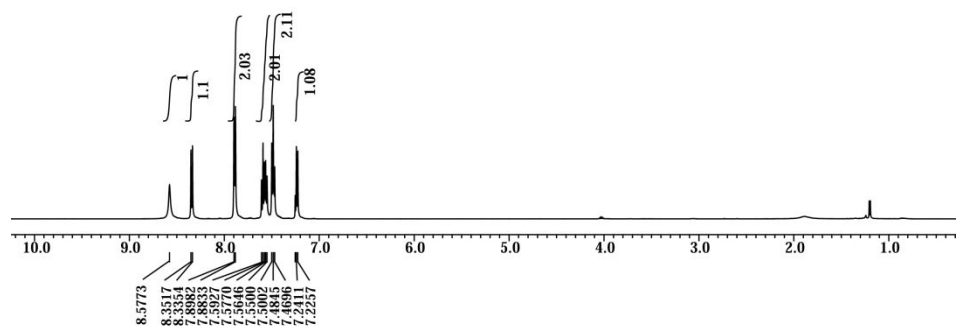
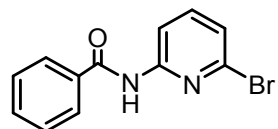
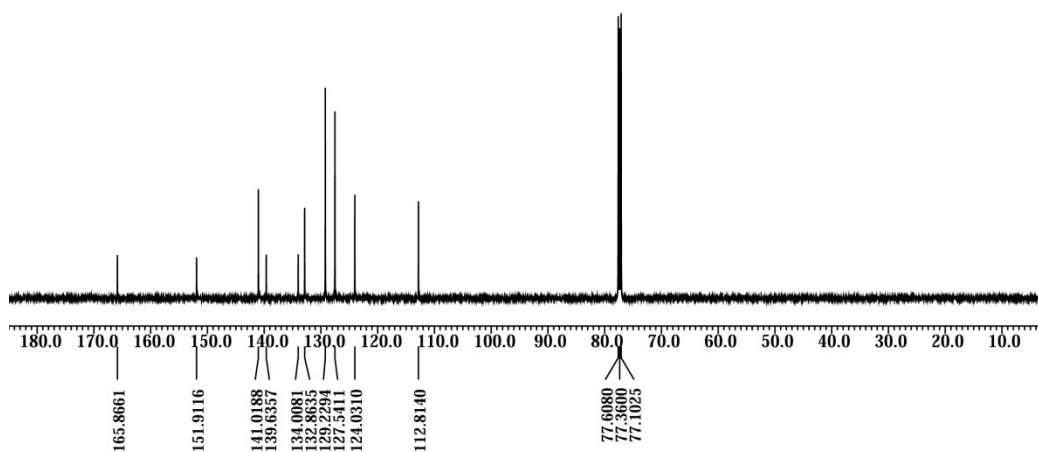


Figure S1. Molecular structure of the cationic unit of $[L^1H_2]I$.

Spectroscopy Data:**Figure S2.** ^1H NMR of $[\text{L}^{\text{aH}}]$ in CDCl_3 .**Figure S3.** ^{13}C NMR of $[\text{L}^{\text{aH}}]$ in CDCl_3 .

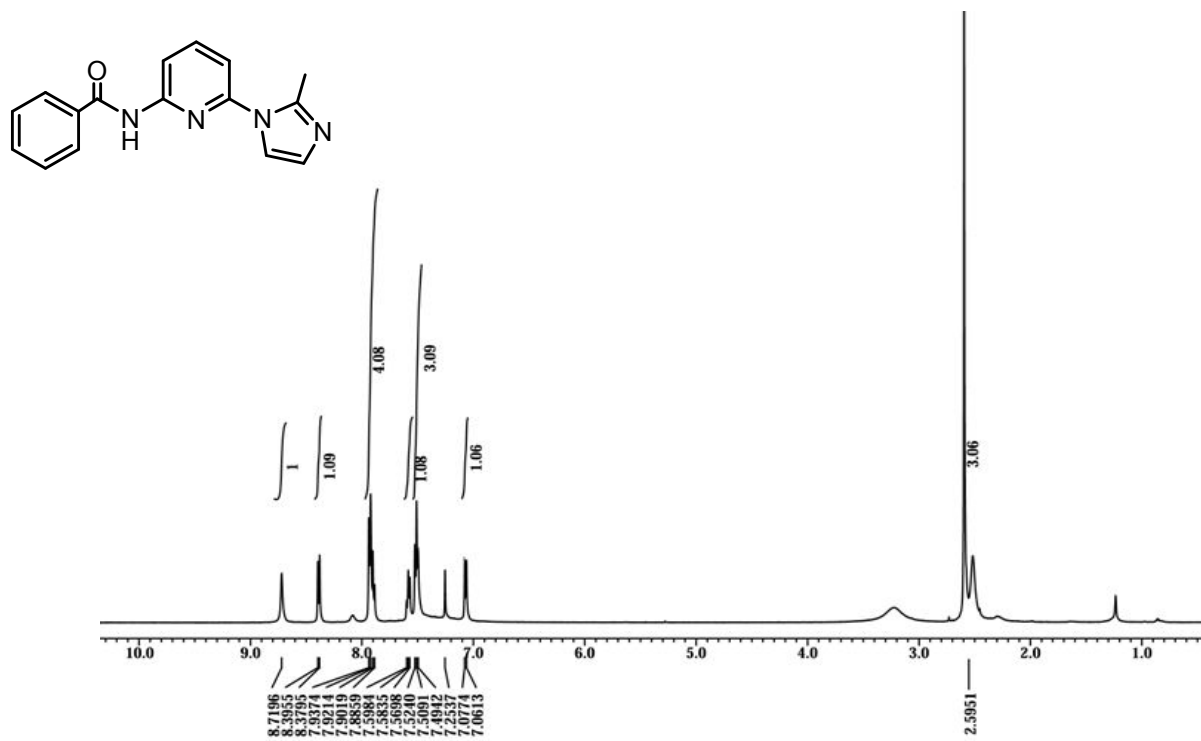


Figure S4. ^1H NMR of $[L^bH_2]$ in CDCl_3 .

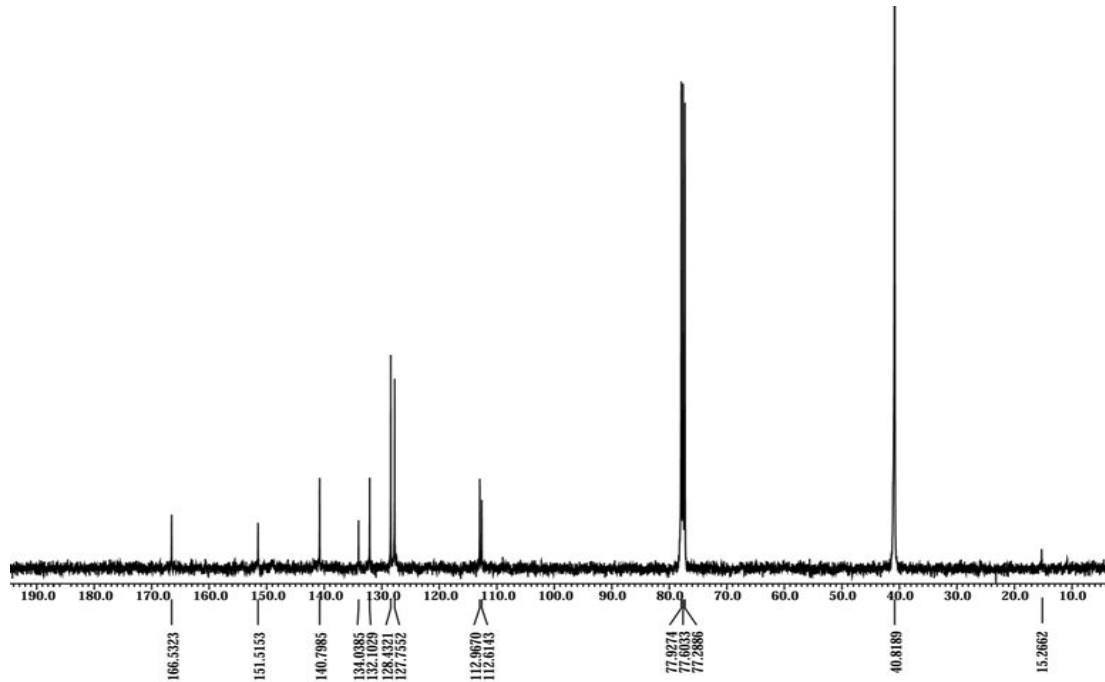


Figure S5. ^{13}C NMR of $[L^bH_2]$ in CDCl_3 .

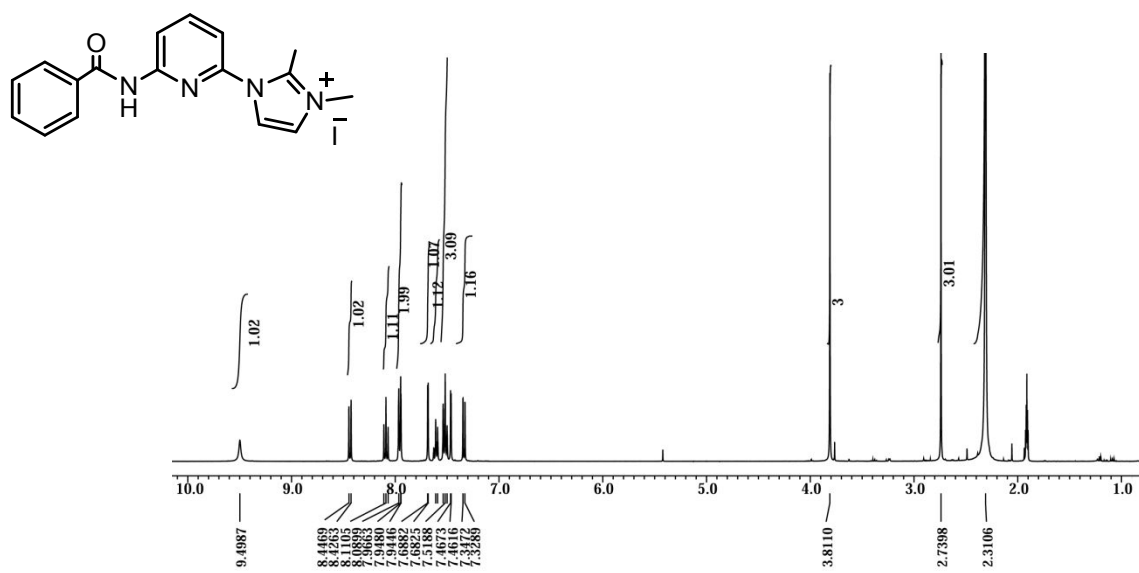


Figure S6. ^1H NMR of $[L^1H_2]^+$ in CD_3CN .

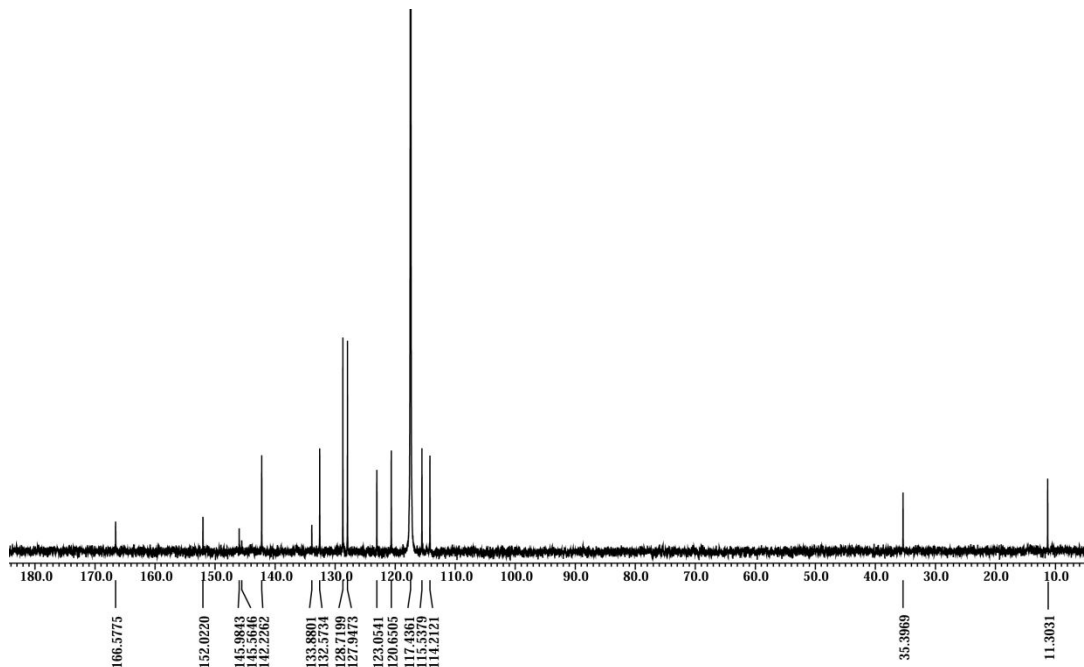


Figure S7. ^{13}C NMR of $[L^1H_2]^+$ in CD_3CN .

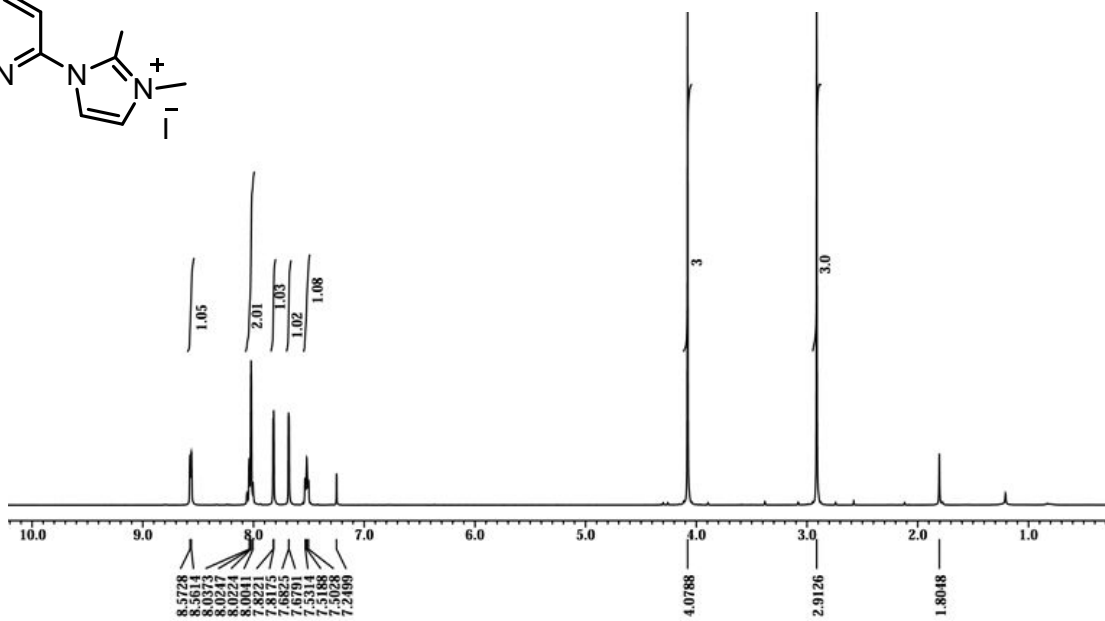
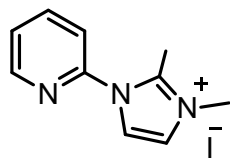


Figure S8. ¹H NMR of $[L^2H]^+$ in $CDCl_3$.

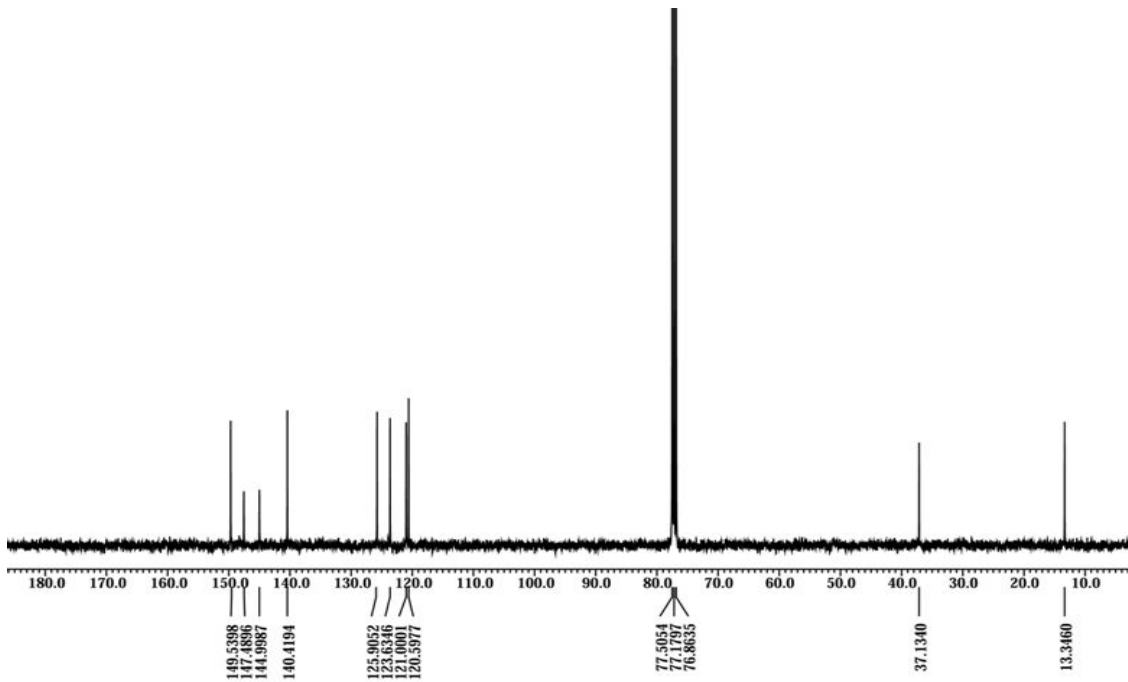


Figure S9. ¹³C NMR spectrum for $[L^2H]^+$ in $CDCl_3$.

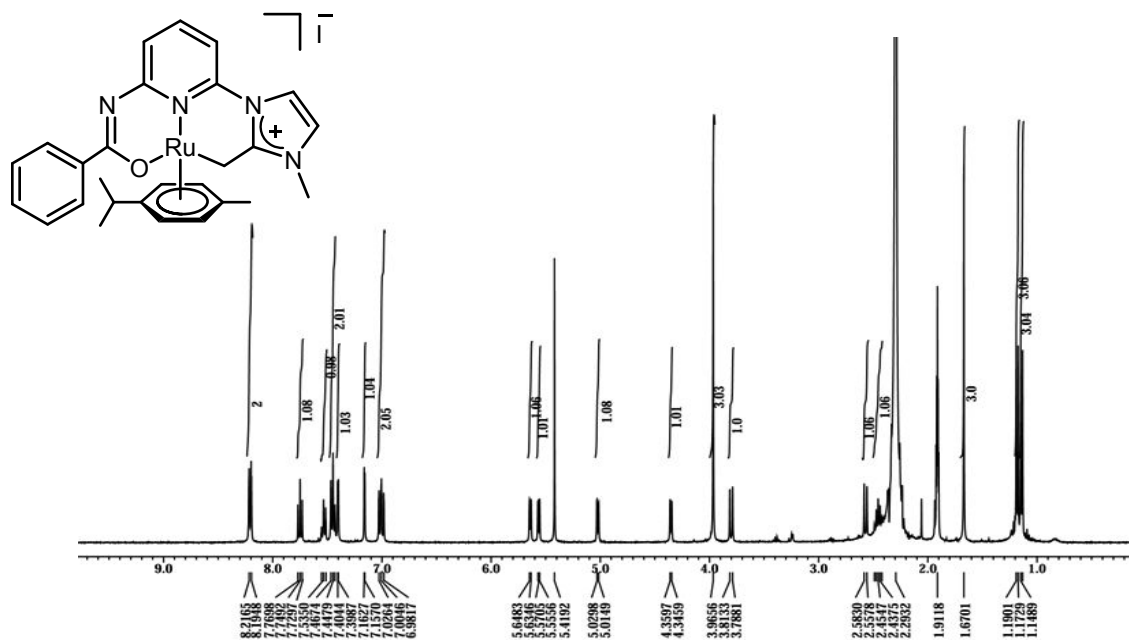


Figure S10. ^1H NMR of **1** in CD_3CN .

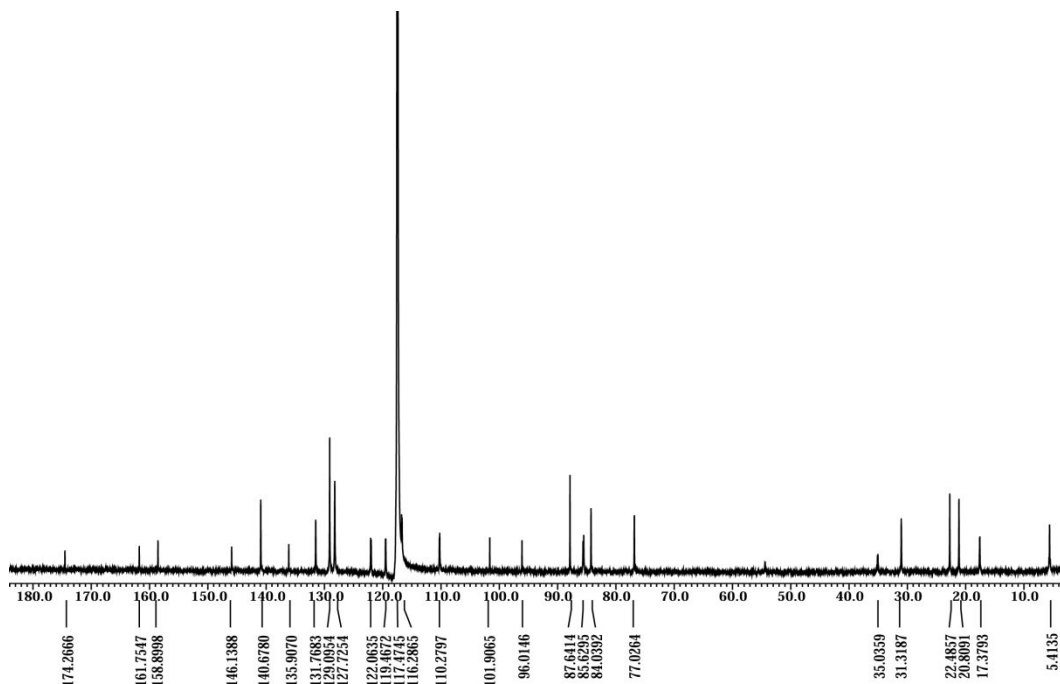


Figure S11. ^{13}C NMR of **1** in CD_3CN .

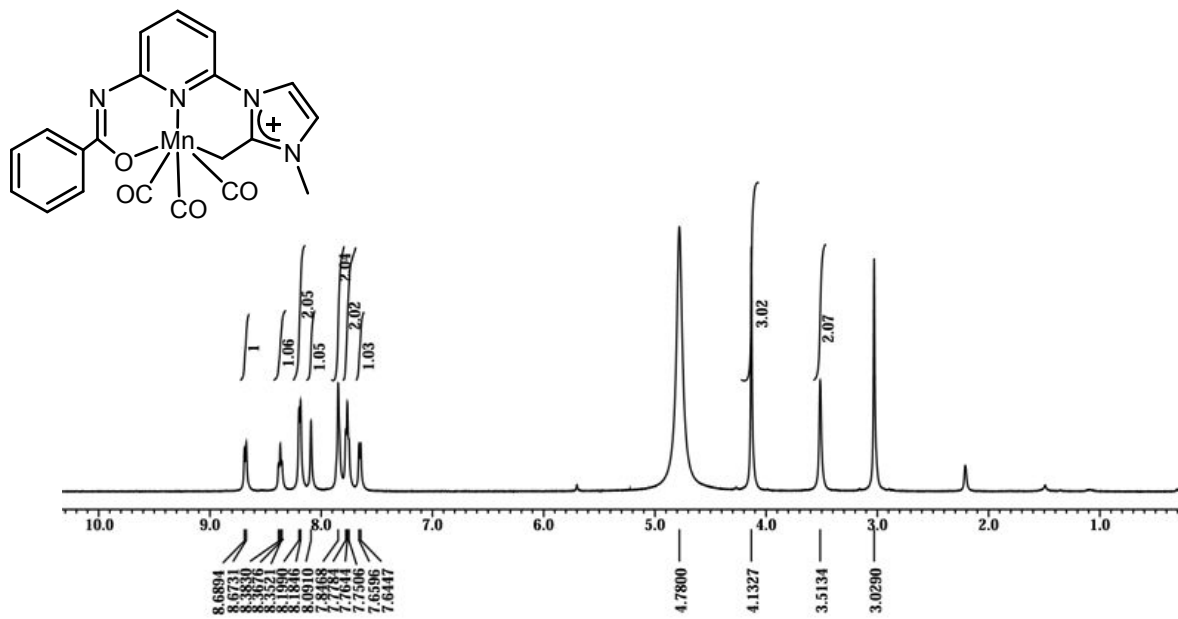


Figure S12. ¹H NMR of **2** in CD₃OD.

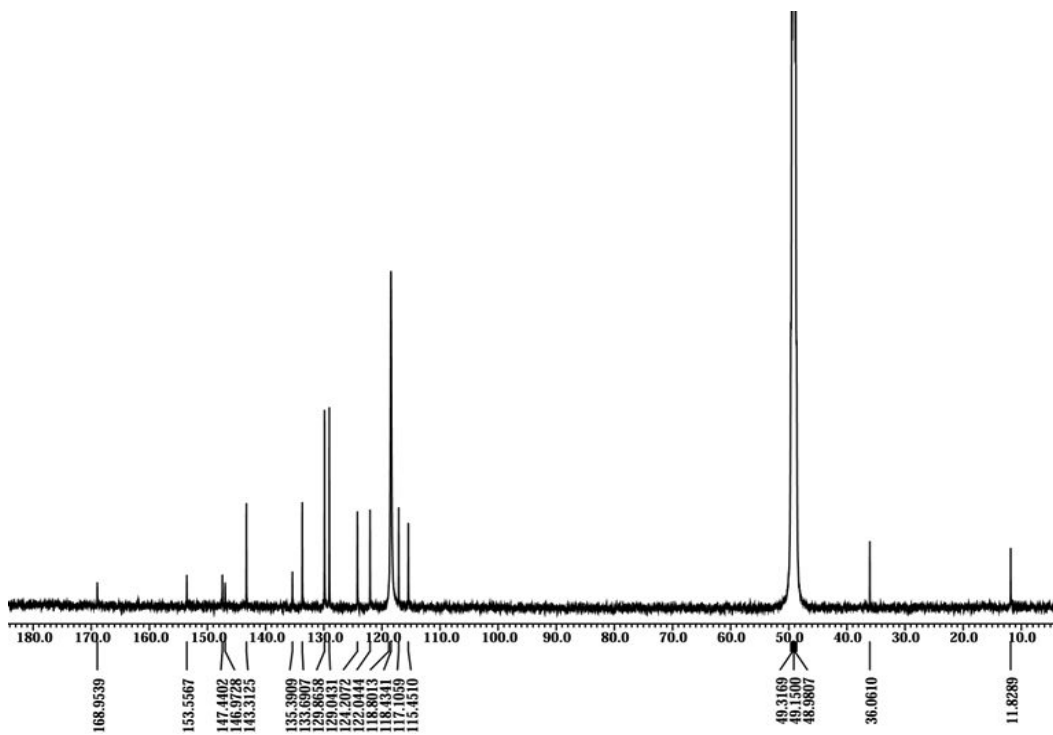


Figure S13. ¹³C NMR of **2** in CD₃OD.

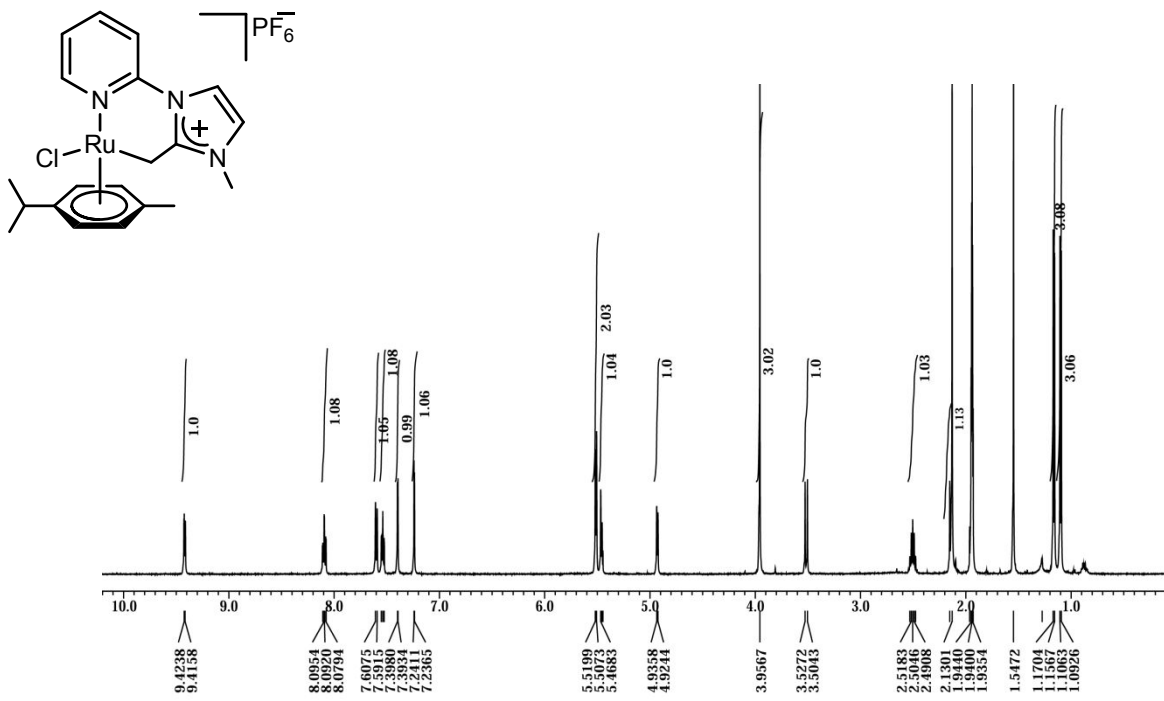


Figure 14. ¹H NMR of 3 in CD₃CN.

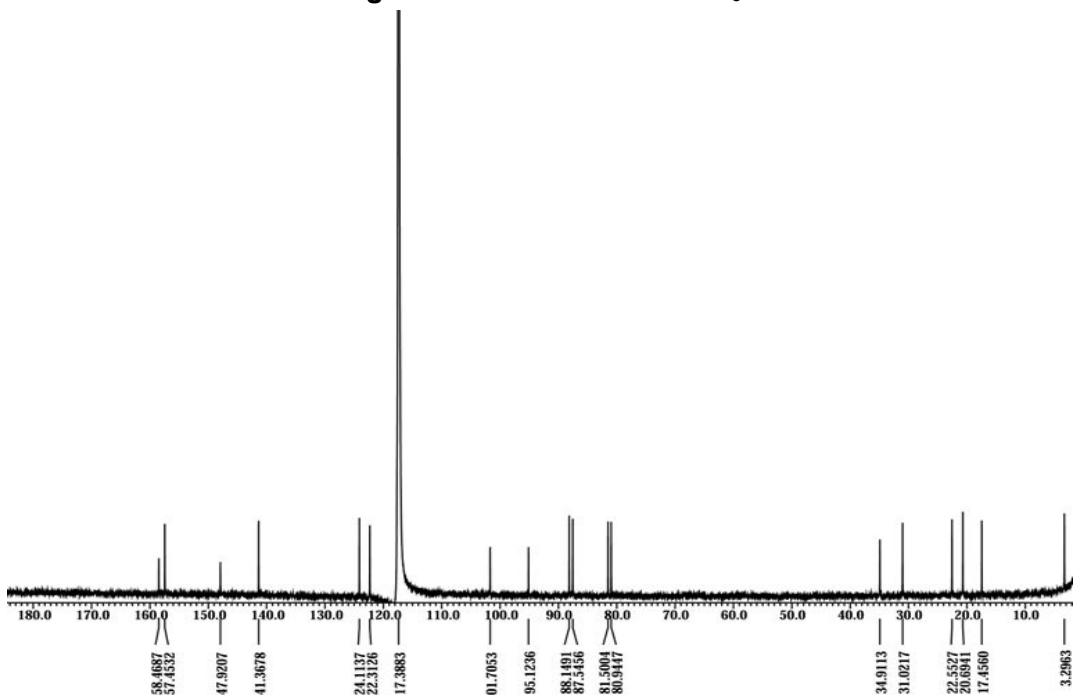


Figure S15. ¹³C NMR of 3 in CD₃CN.

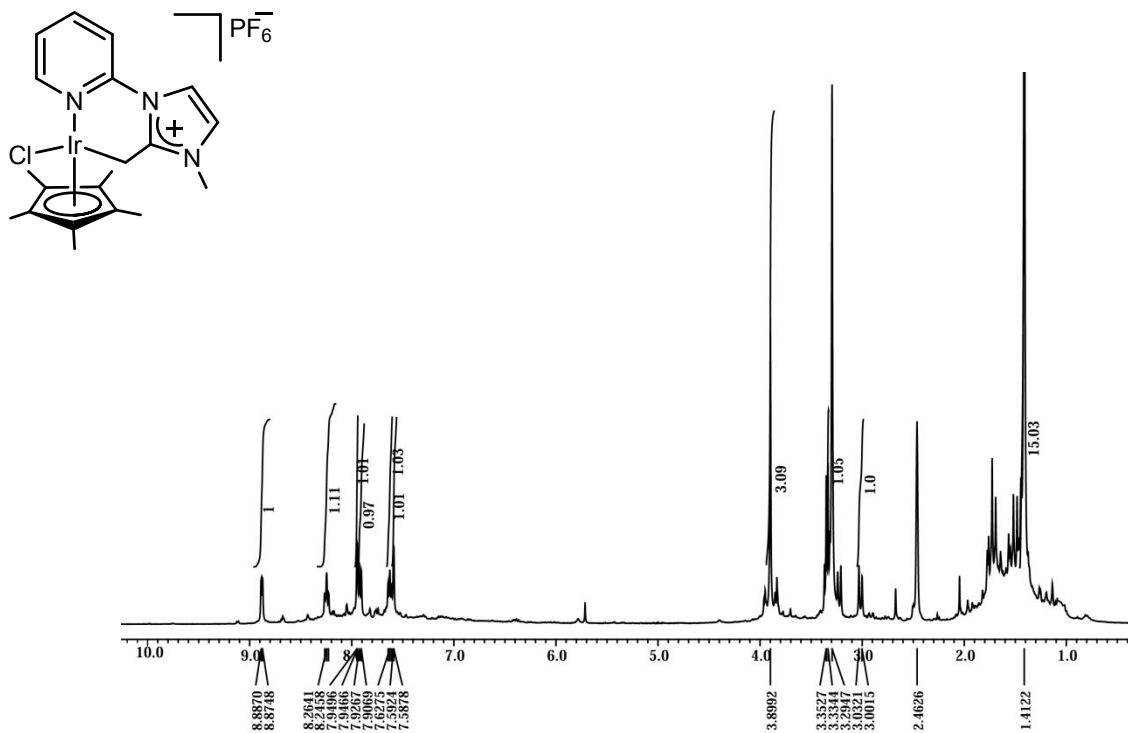


Figure 16. ^1H NMR of **4** in $\text{DMSO}-\text{d}_6$.

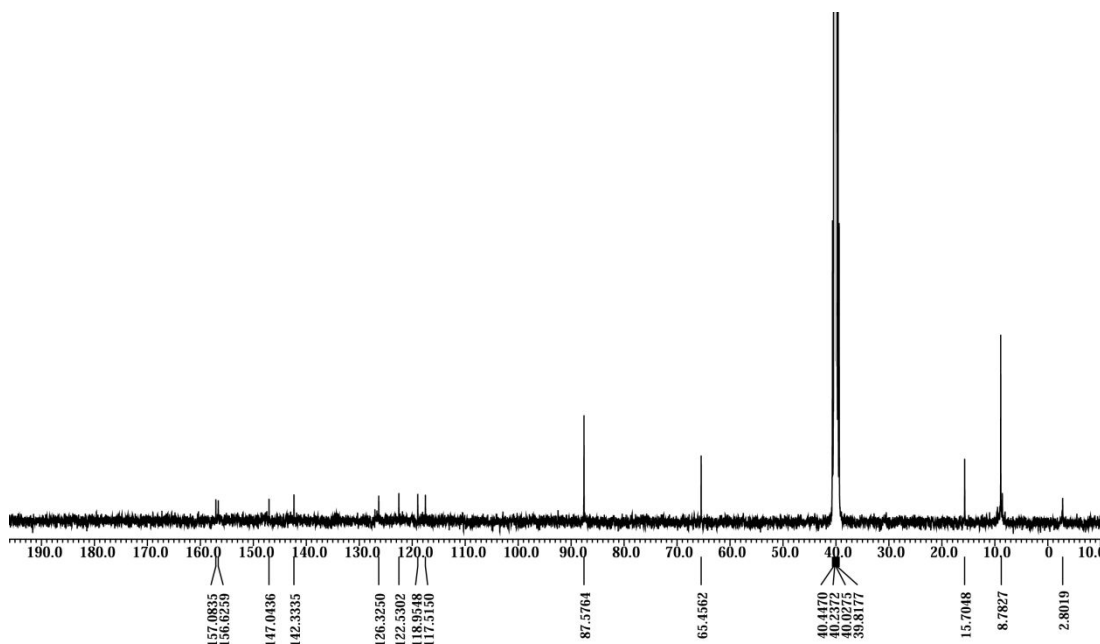


Figure 17. ^{13}C NMR of **4** in $\text{DMSO}-\text{d}_6$.

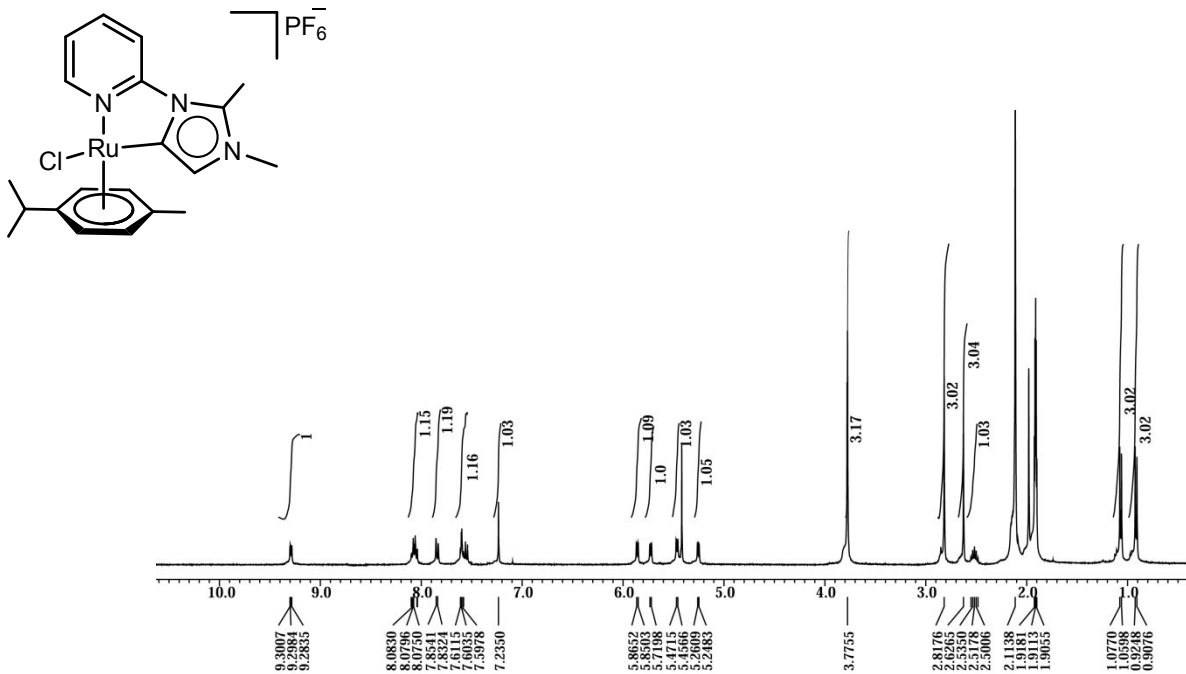


Figure S18. ^1H NMR of **5** in CD_3CN .

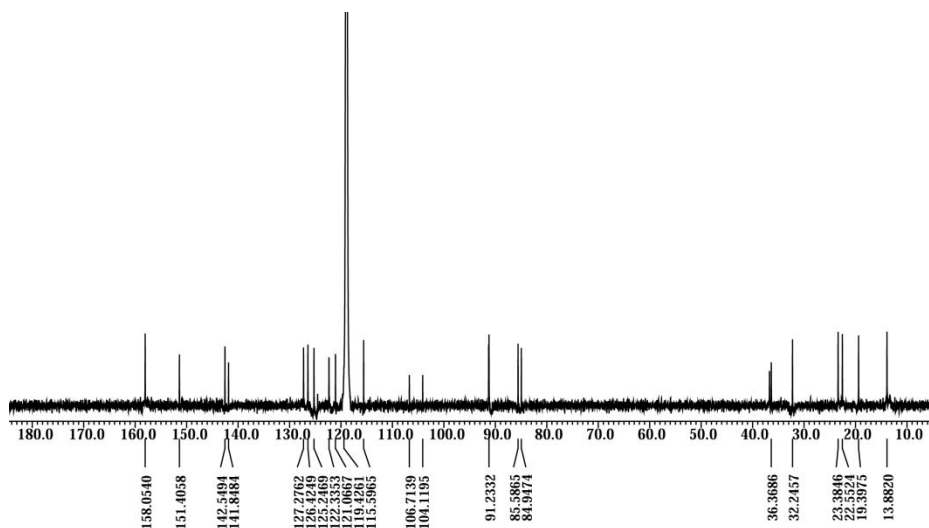


Figure S19. ^{13}C NMR of **5** in CD_3CN .

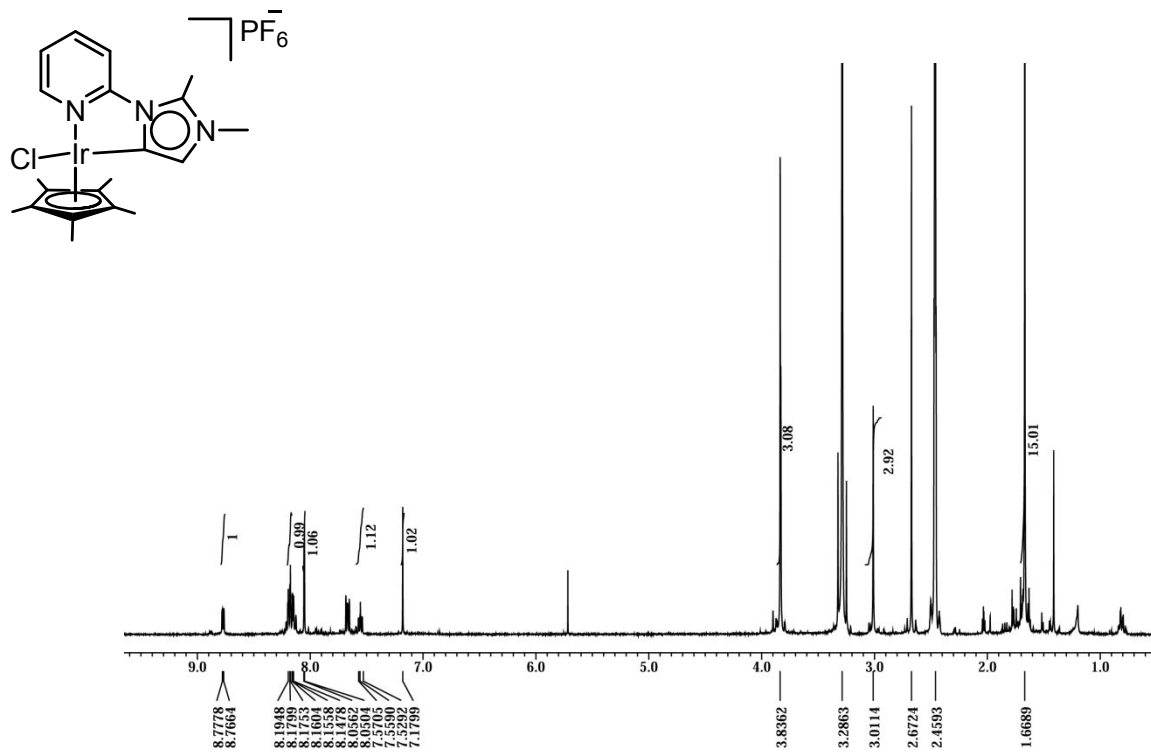


Figure S20. ^1H NMR of **6** in $\text{DMSO}-\text{d}_6$.

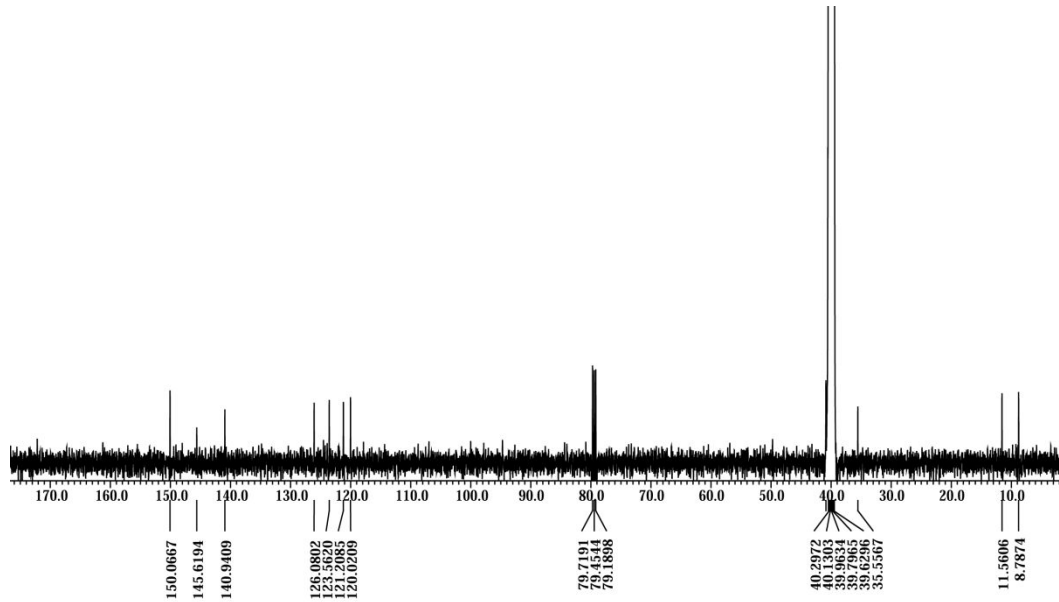


Figure S21. ^{13}C NMR of **6** in CD_3OD .

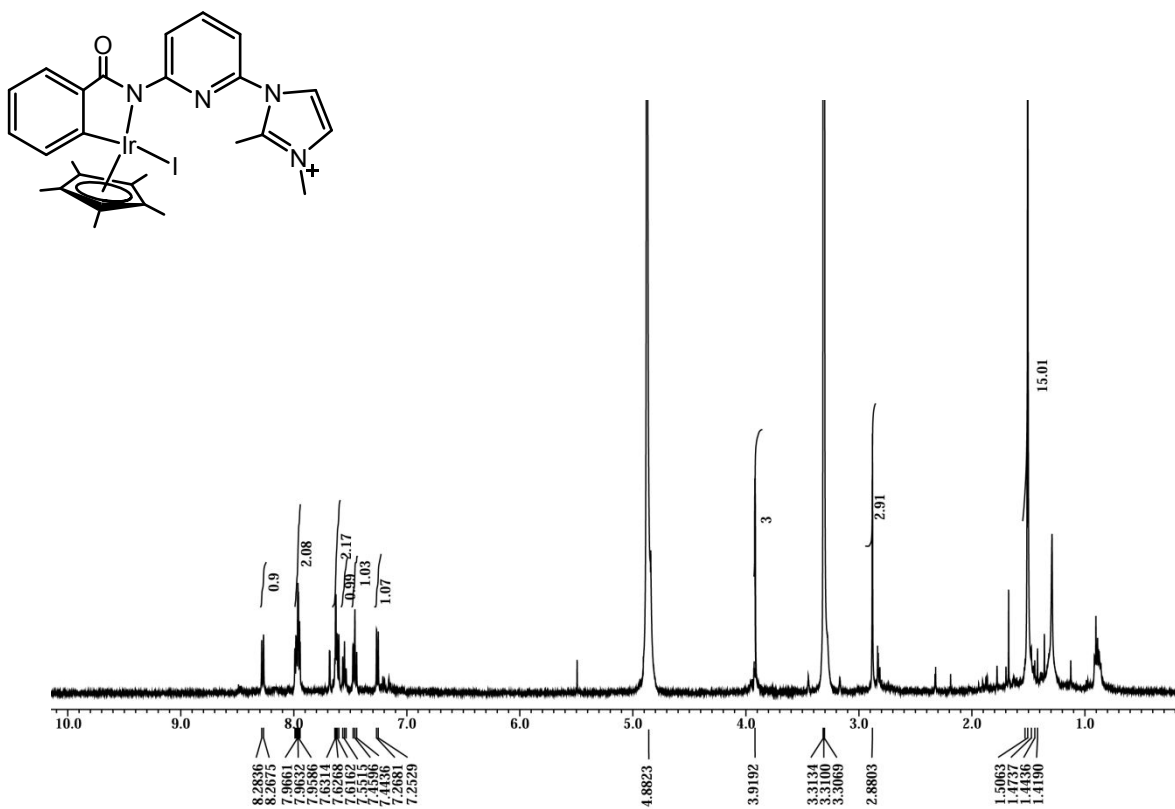


Figure S22. ¹H NMR of 7 in CD₃OD.

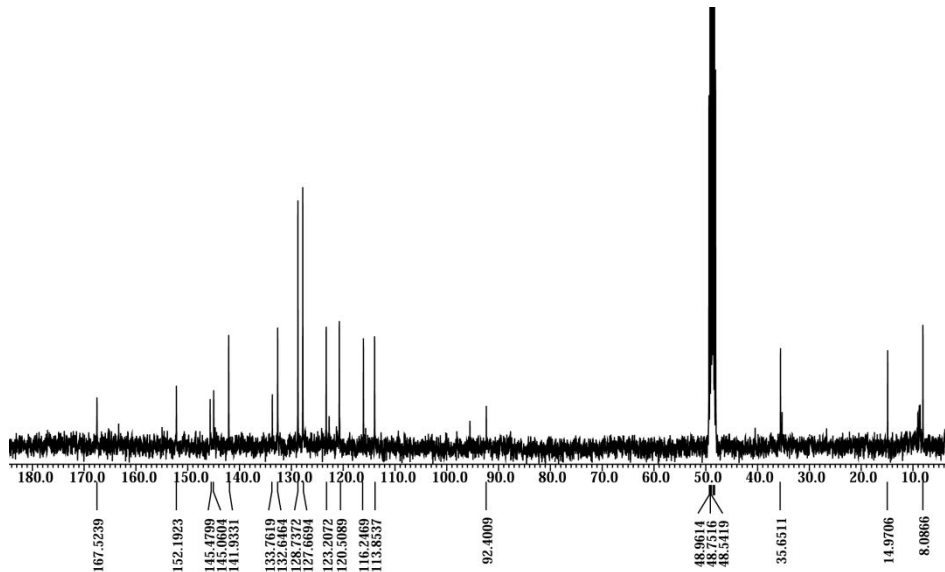


Figure S23. ¹³C NMR of 7 in CD₃OD.

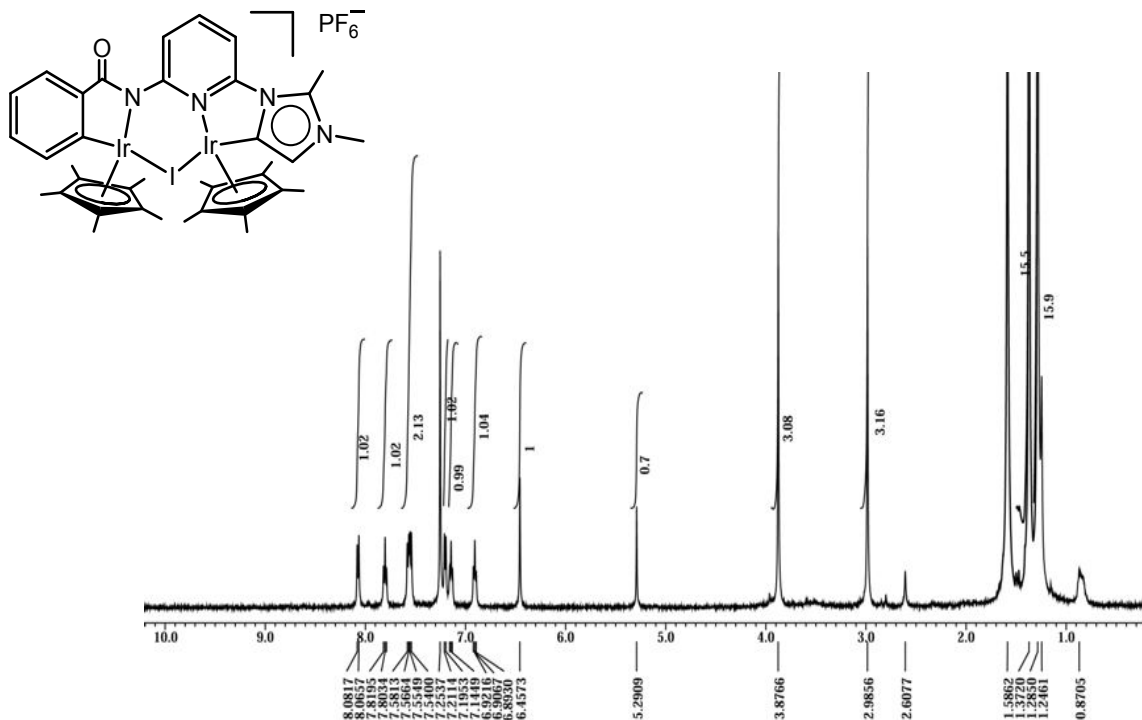


Figure S24. ^1H NMR of **8** in CDCl_3 .

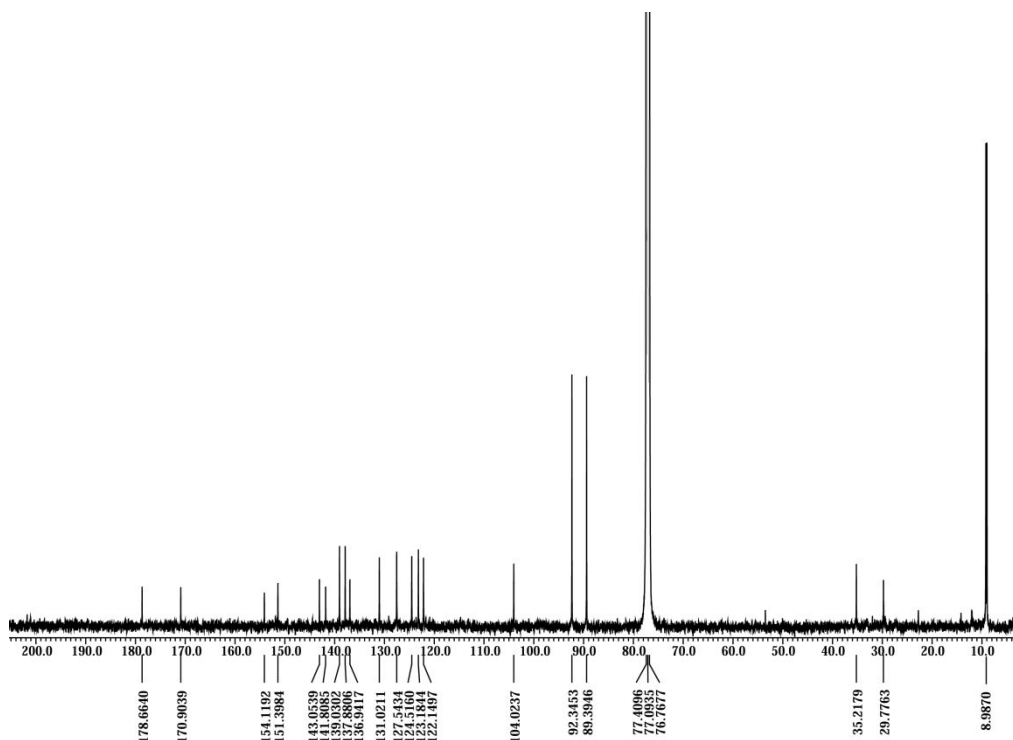


Figure S25. ^{13}C NMR of **8** in CDCl_3 .

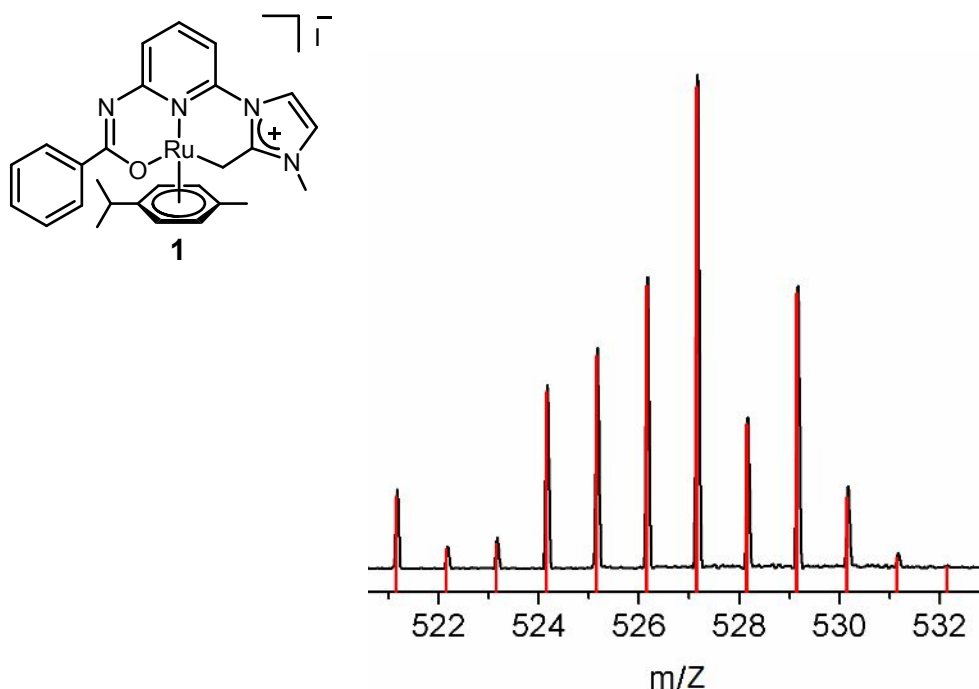


Figure S26. Experimental (black) and simulated (red) ESI-MS of $[1 - I]^+$.

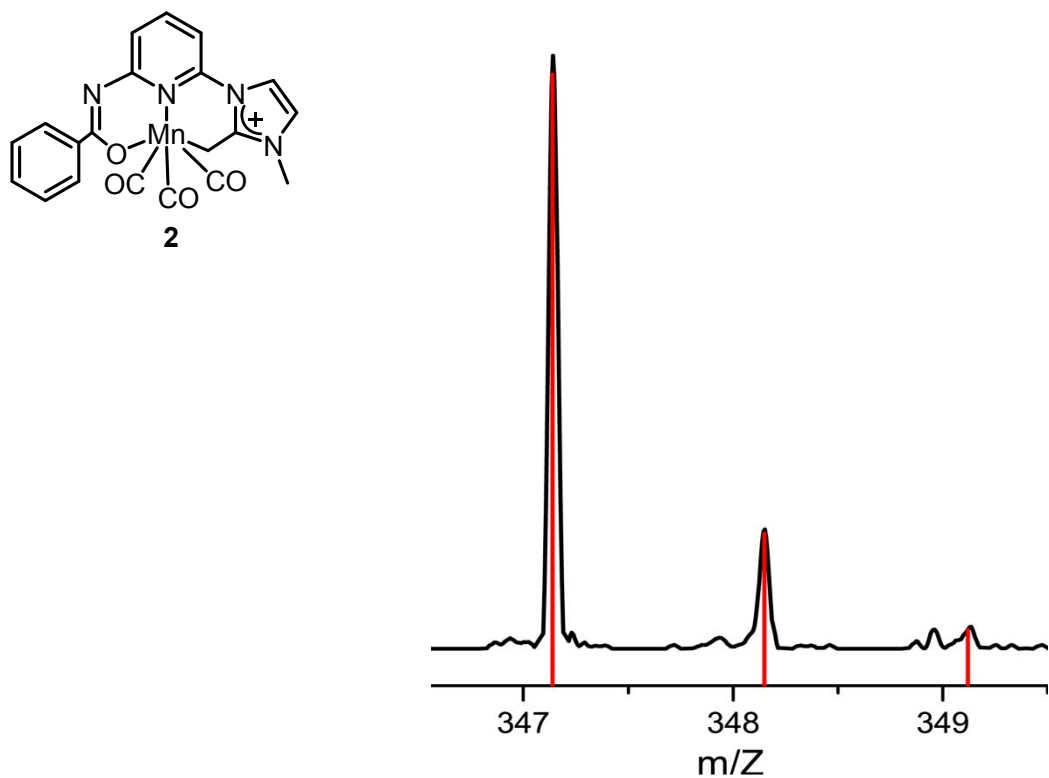


Figure S27. Experimental (black) and simulated (red) ESI-MS of $[2 - 3\text{CO} + \text{H}]^+$.

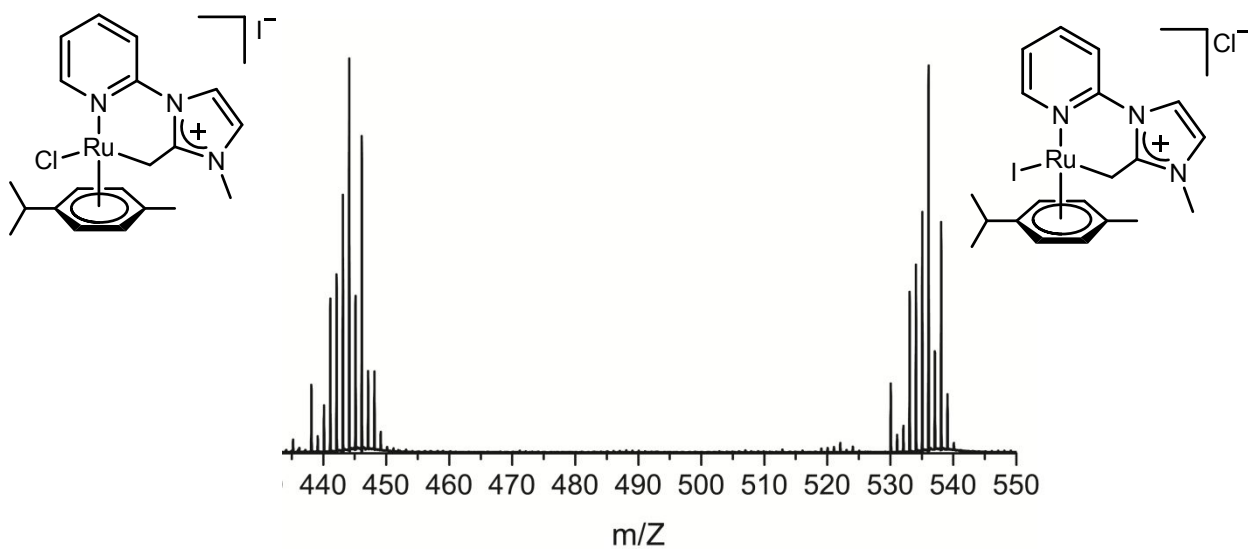


Figure S28. ESI-MS spectrum of $[\text{RuL}^2(\text{p-cymene})\text{Cl}]^+$ (left) and $[\text{RuL}^2(\text{p-cymene})\text{I}]^+$ (right).

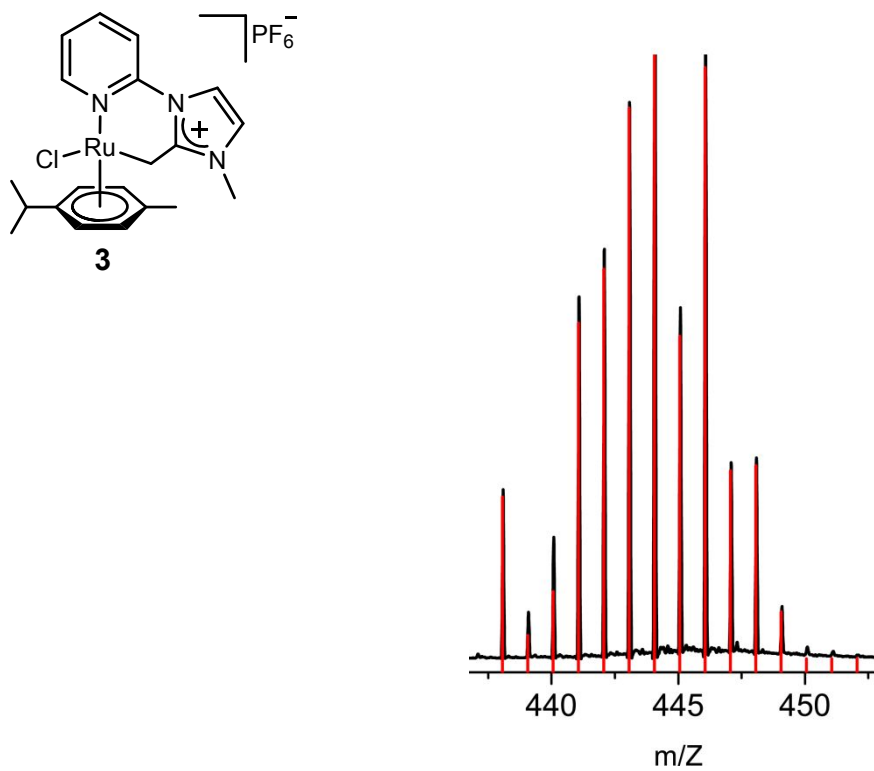


Figure S29 Experimental (black) and simulated (red) ESI-MS spectrum of $[\mathbf{3}-\text{PF}_6]^+$.

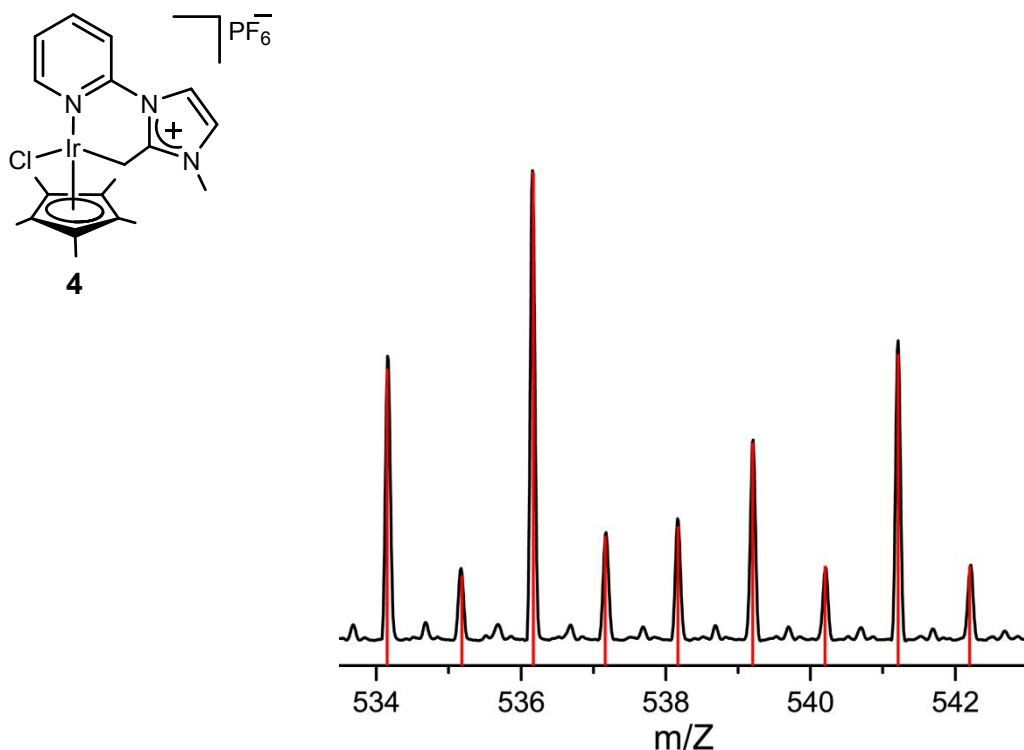


Figure S30. Experimental (black) and simulated (red) ESI-MS spectrum of $[\mathbf{4} - \text{PF}_6]^{+}$.

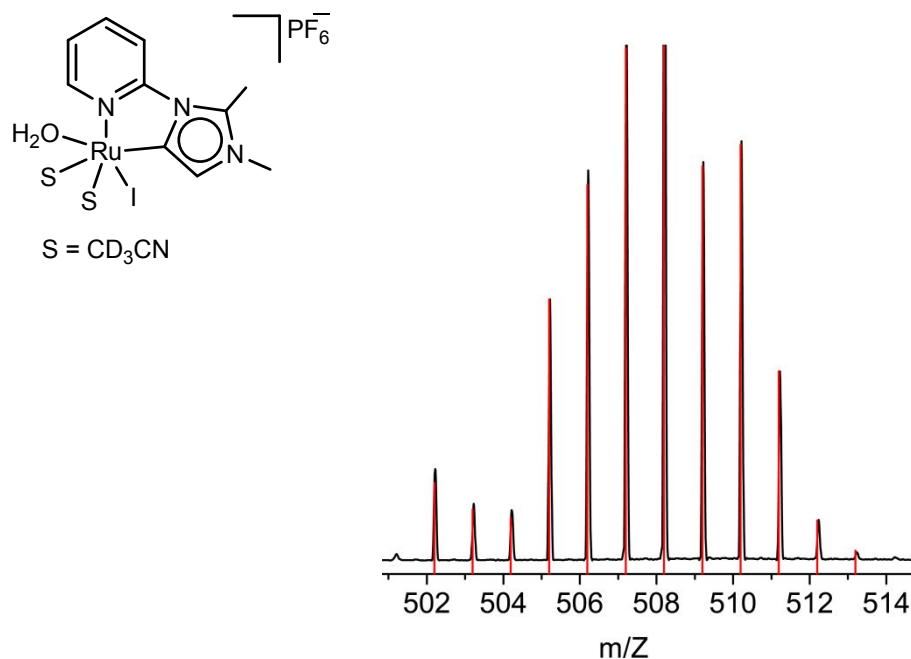


Figure S31. Experimental (black) and simulated (red) ESI-MS spectrum of $[\text{RuL}^2(\text{CD}_3\text{CN})_2(\text{H}_2\text{O})\text{I}]^{+}$.

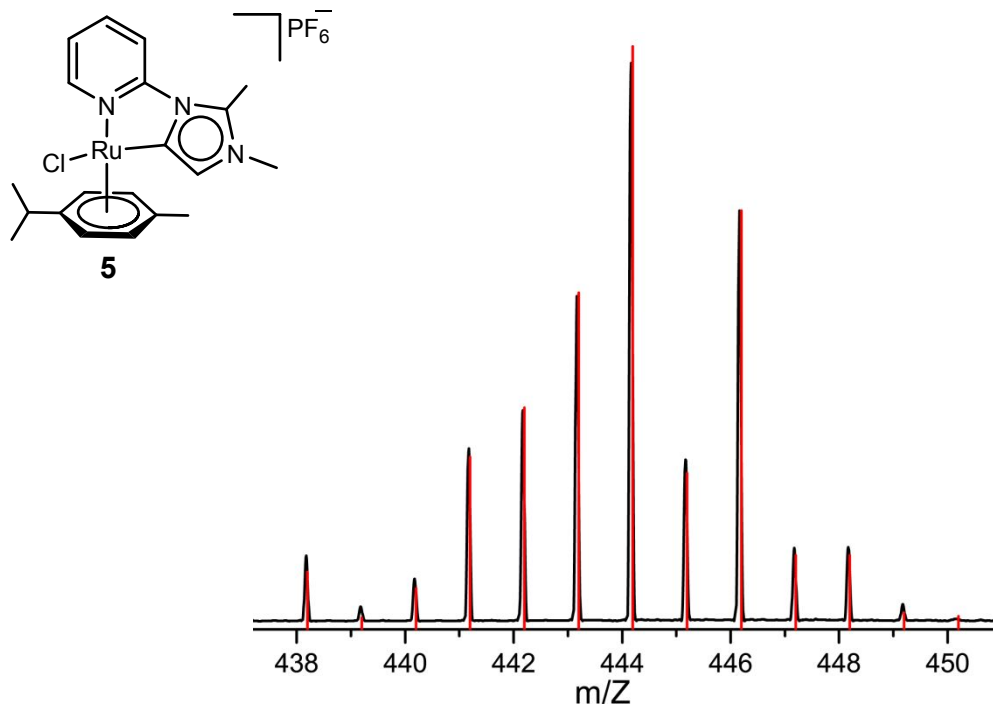


Figure S32. Experimental (black) and simulated (red) ESI-MS spectrum of $[5 - \text{PF}_6]^{+}$.

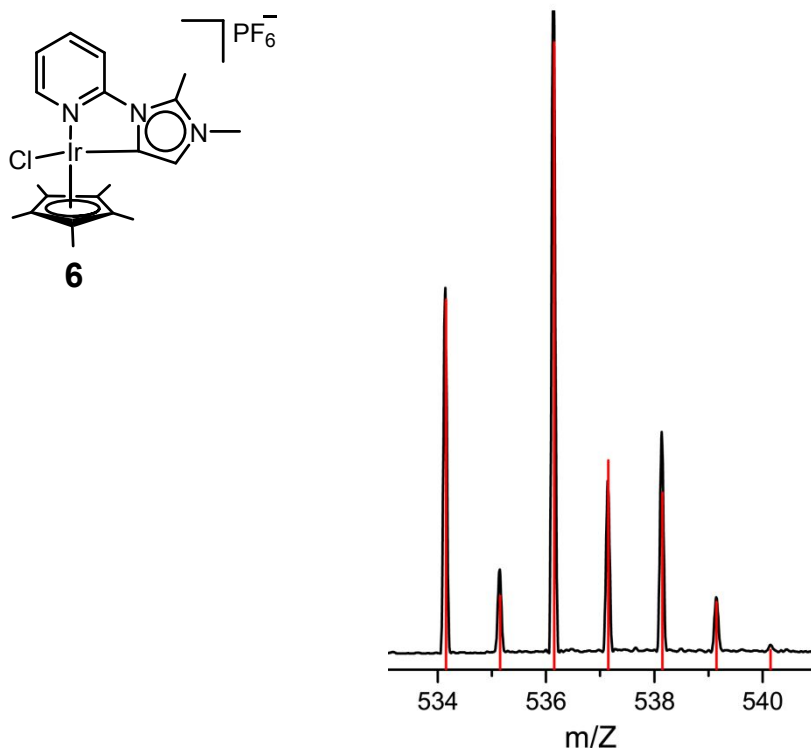


Figure S33 Experimental (black) and simulated (red) ESI-MS spectrum of $[6 - \text{PF}_6]^{+}$.

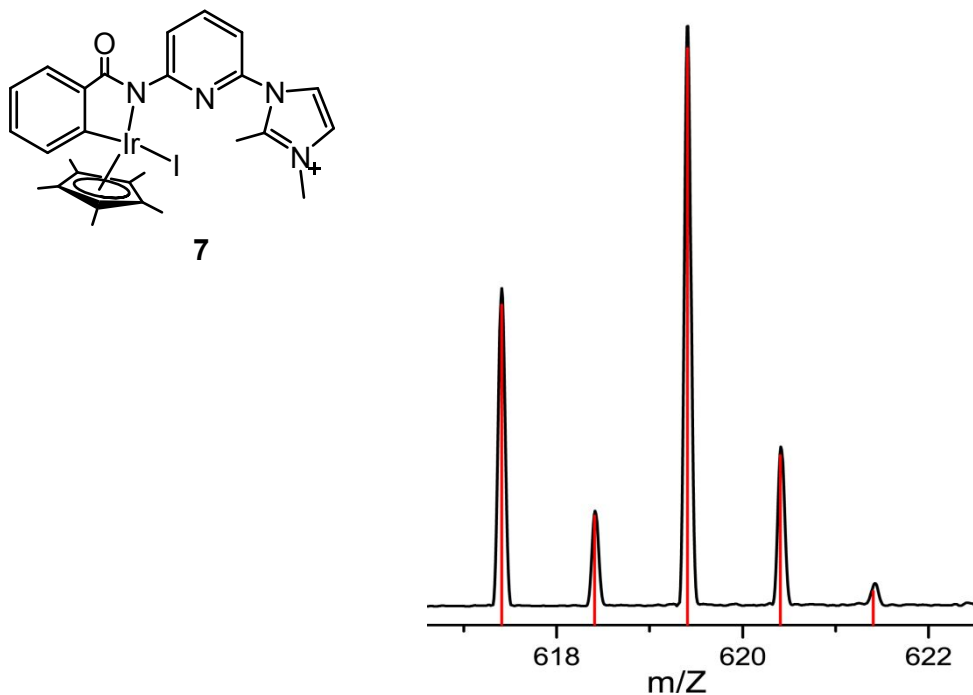


Figure S34. Experimental (black) and simulated (red) ESI-MS spectrum of $[7 - I]^+$.

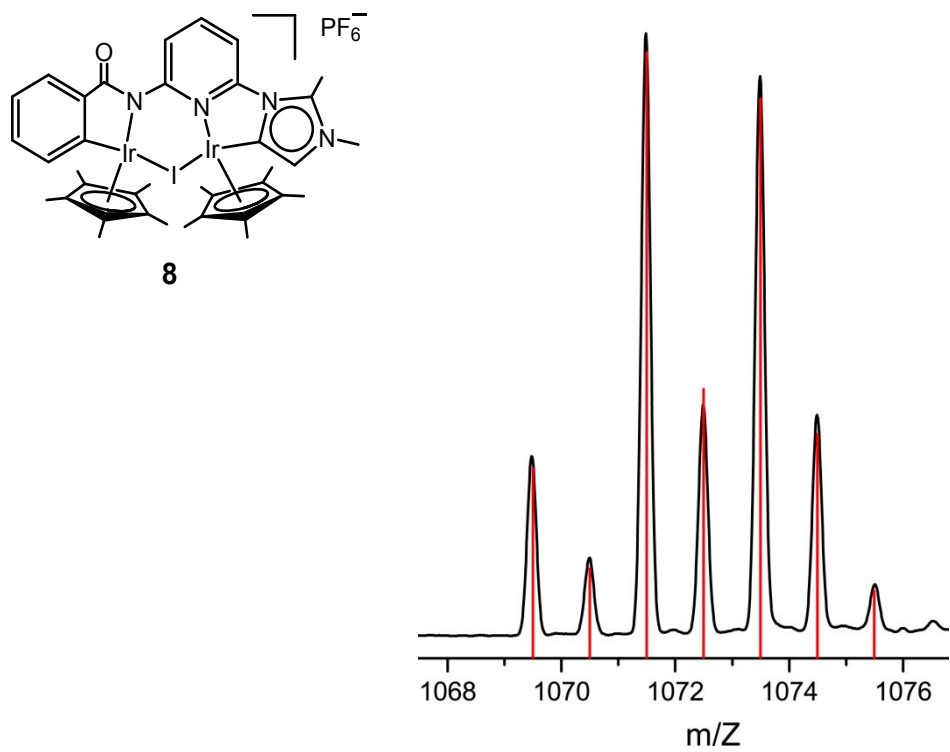


Figure S35. Experimental (black) and simulated (red) ESI-MS spectrum of $[8 - \text{PF}_6]^+$.

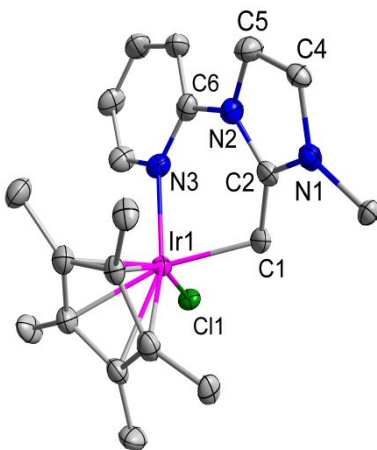


Figure S36. Molecular structure of the cationic unit of **4** with important atoms labeled. All hydrogens are omitted for the sake of clarity. Selected bond lengths (\AA) and angles ($^{\circ}$): Ir1–C1 2.115(4), Ir1–N3 2.110(4), Ir1–Cl 2.4042(11), N3–Ir1–C1 83.13(17), Ir1–C1–C2 107.1(3).

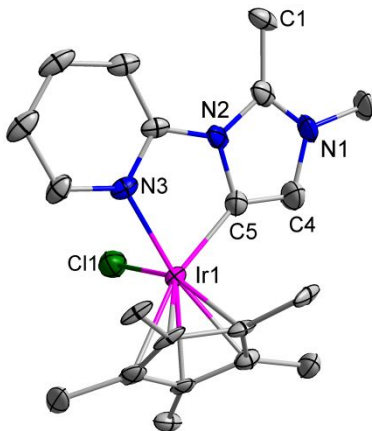


Figure S37. Molecular structure of the cationic unit of **6** with important atoms labeled. All hydrogens are omitted for the sake of clarity. Selected bond lengths (\AA) and angles ($^{\circ}$): Ir1–C5 2.006(9), Ir1–N3 2.087(7), Ir1–Cl1 2.5200(18), N3–Ir1–C5 76.9(3).

Table S1. Crystallographic Data and Pertinent Refinement Parameters for **1**, **2**, **3** and **5**

	1.CH₂Cl₂	2	3	5.CH₂Cl₂
Empirical formula	C ₂₈ H ₂₇ N ₄ OICl ₂ Ru ₁	C ₂₂ H ₁₅ N ₃ O ₄ Mn ₁	C ₂₀ H ₂₅ ClF ₆ N ₃ PRu ₁	C ₂₁ H ₂₇ Cl ₃ N ₃ F ₆ PRu ₁
Formula Weight	734.40	428.04	588.92	673.84
Crystal System	Monoclinic	Orthorhombic	Orthorhombic	Monoclinic
Space Group	<i>P2(1)/c</i>	<i>Pbca</i>	<i>Pbcm</i>	<i>P121/c1</i>
a (Å)	11.0142(7)	7.9705(5)	19.694(2)	7.8856(5)
b (Å)	19.7894(12)	19.0173(12)	8.8003(11)	10.7768(7)
c (Å)	13.2530(9)	23.8833(16)	12.8643(16)	30.1846(18)
α (deg)	90.00	90.00	90.00	90
β (deg)	94.325(2)	90.00	90.00	94.147(2)
γ (deg)	90.00	90.00	90.00	90
V (Å ³)	2880.5(3)	3620.2(4)	2229.5(5)	2558.4(3)
Z	4	8	4	4
ρ _{calcd} (g cm ⁻³)	1.693	1.579	1.754	1.749
μ (mm ⁻¹)	1.830	0.766	0.958	1.049
F(000)	1448	1760	1184	1352
Reflections				
Collected	28811	26607	32452	39891
Independent	7158	3209	5570	6360
Observed [I > 2σ(I)]	5749	2103	5140	5716
No. of variables	338	263	293	358
GooF	1.023	1.021	1.111	1.048
R _{int}	0.0484	0.1367	0.0507	0.0378
Final R indices	R1 = 0.0386	R1 = 0.0567	R1 = 0.0261	R1 = 0.0307
[I > 2σ(I)] ^a	wR2 = 0.0861	wR2 = 0.1050	wR2 = 0.0594	wR2 = 0.0744
R indices (all data) ^a	R1 = 0.0567	R1 = 0.1080	R1 = 0.0314	R1 = 0.0361
	wR2 = 0.0925	wR2 = 0.1221	wR2 = 0.0700	wR2 = 0.0785

^aR₁ = Σ ||F_o| - |F_c| / Σ |F_o| with F_o² > 2σ(F_o²). wR₂ = [Σw(|F_o²| - |F_c²|)² / Σ |F_o²|²]^{1/2}

Table S2. Crystallographic Data and Pertinent Refinement Parameters for **7**, **8** and **[L¹H₂]I**

	7.CH₂Cl₂.H₂O	8.CH₂Cl₂	[L¹H₂]I
Empirical formula	C ₂₈ H ₃₄ Cl ₂ N ₄ O ₂ Ir ₁	C ₇₅ H ₈₈ Cl ₂ F ₁₂ I ₂ N ₈ O ₂ P ₂ Ir ₄	C ₁₇ H ₁₆ N ₄ O ₁
Formula Weight	848.59	2516.97	419.24
Crystal System	Triclinic	Orthorhombic	Monoclinic
Space Group	<i>P</i> -1	<i>Pna</i> 21	<i>P2(1)/c</i>
a (Å)	9.1694(6)	16.823(13)	13.1794(7)
b (Å)	10.7369(7)	10.9581(8)	7.0717(4)
c (Å)	15.2555(10)	43.218(3)	18.3002(10)
α (deg)	83.758(10)	90.00	90
β (deg)	84.308(10)	90.00	100.693(2)
γ (deg)	74.161(10)	90.00	90
V (Å ³)	1432.53(16)	7967.4(10)	1675.98(16)
Z	2	4	4
ρ _{calcd} (g cm ⁻³)	1.967	2.098	1.662
μ (mm ⁻¹)	5.958	7.621	1.920
F(000)	820	4784	828.0
Reflections			
Collected	16891	71312	24649
Independent	7114	19372	4162
Observed [I > 2σ(I)]	6659	15760	3426
No. of variables	348	938	210
GooF	1.031	1.035	1.112
R _{int}	0.0236	0.0715	0.0567
Final R indices	R1 = 0.0215	R1 = 0.0459	0.0394
[I > 2σ(I)] ^a	wR2 = 0.0503	wR2 = 0.0958	0.0697
R indices (all data) ^a	R1 = 0.0242	R1 = 0.0665	0.0550
	wR2 = 0.0513	wR2 = 0.1025	0.0761

^aR₁ = Σ ||F_o| - |F_c|| / Σ |F_o| with F_o² > 2σ(F_o²). wR₂ = [Σ w(|F_o²| - |F_c²|)² / Σ |F_o²|²]^{1/2}

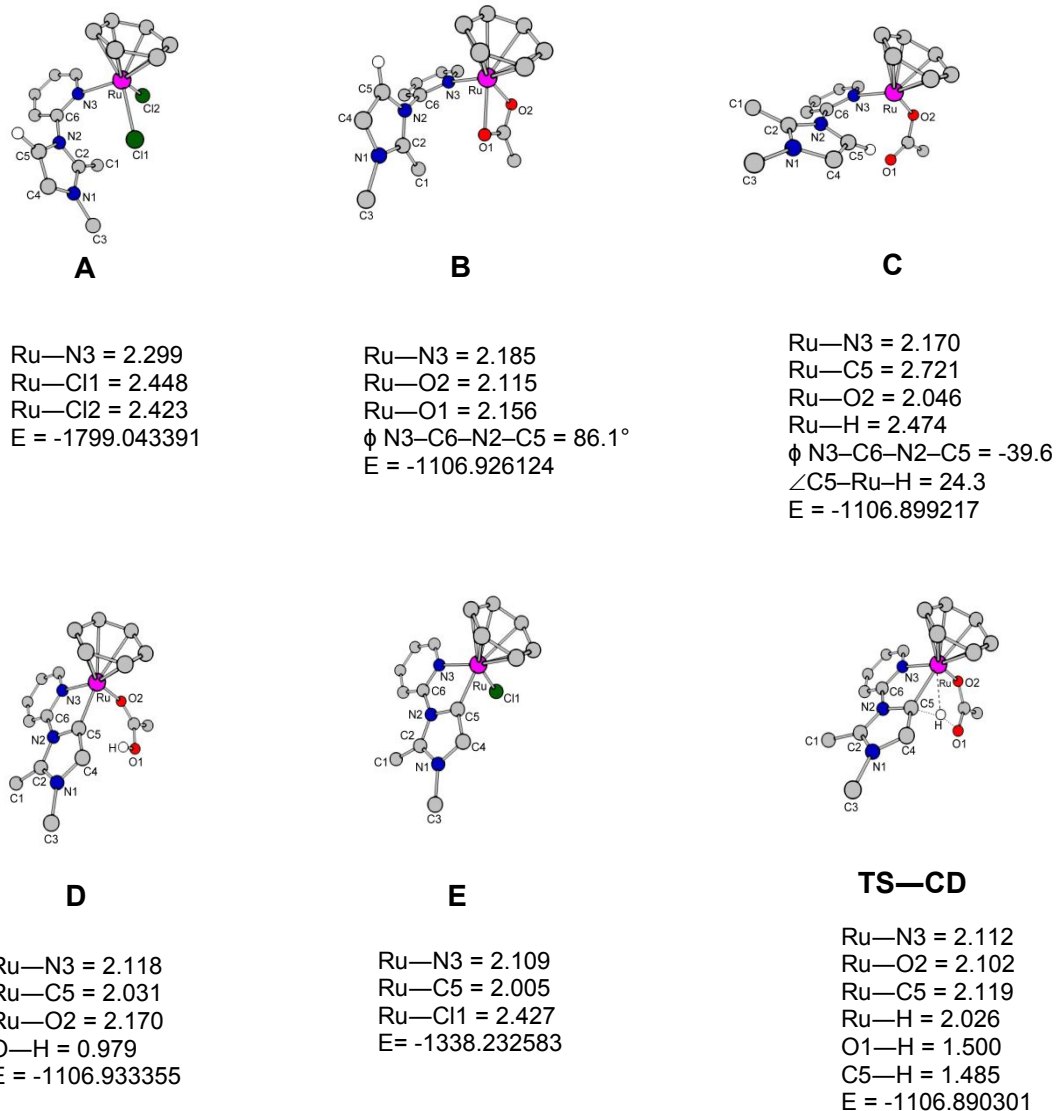


Figure S38. Optimized structures of the intermediates and the transition state (TS). Selected bond lengths (\AA), bond angles ($^\circ$) and energies (RB3LYP, Hartree) are given below each structure.